



# Chemistry A European Journal

 **Chemistry  
Europe**  
European Chemical  
Societies Publishing

## Accepted Article

**Title:** Triphenylphosphine-Based Covalent Organic Frameworks and Heterogeneous Rh-P-COFs Catalysts

**Authors:** Yubing Liu, Alla Dikhtiarenko, Naizhang Xu, Jiawei Sun, Jie Tang, Kaiqiang Wang, Bolian Xu, Qing Tong, Hero Jan Heeres, Songbo He, Jorge Gascon, and Yining Fan

This manuscript has been accepted after peer review and appears as an Accepted Article online prior to editing, proofing, and formal publication of the final Version of Record (VoR). This work is currently citable by using the Digital Object Identifier (DOI) given below. The VoR will be published online in Early View as soon as possible and may be different to this Accepted Article as a result of editing. Readers should obtain the VoR from the journal website shown below when it is published to ensure accuracy of information. The authors are responsible for the content of this Accepted Article.

**To be cited as:** *Chem. Eur. J.* 10.1002/chem.202002150

**Link to VoR:** <https://doi.org/10.1002/chem.202002150>

WILEY-VCH

## RESEARCH ARTICLE

## Triphenylphosphine-Based Covalent Organic Frameworks and Heterogeneous Rh-P-COFs Catalysts

Yubing Liu<sup>[a]</sup>, Alla Dikhtiarenko<sup>[b]</sup>, Naizhang Xu<sup>[a]</sup>, Jiawei Sun<sup>[a]</sup>, Jie Tang<sup>[a]</sup>, Kaiqiang Wang<sup>[a]</sup>, Bolian Xu<sup>[a]</sup>, Qing Tong<sup>[a]</sup>, Hero Jan Heeres<sup>[c]</sup>, Songbo He<sup>\*,[c]</sup>, Jorge Gascon<sup>\*,[b]</sup> and Yining Fan<sup>\*,[a]</sup>

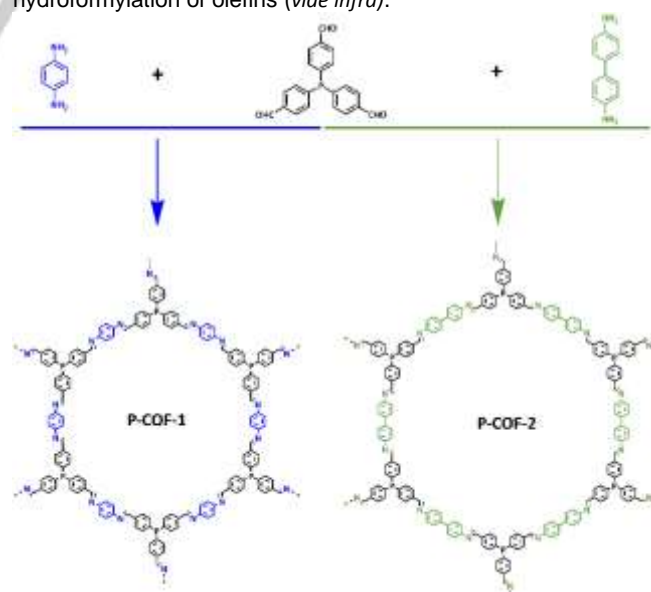
**Abstract:** The synthesis of phosphine-based functional covalent organic frameworks (COFs) has attracted great attention recently. Here, we present two examples of triphenylphosphine-based COFs (termed as P-COFs) with well-defined crystalline structures, high specific surface areas and good thermal stability. Furthermore, the rhodium catalysts using the obtained P-COFs as support materials show high turnover frequency (TOF) for the hydroformylation of olefins, as well as the excellent recycling performance. This work not only extended phosphine-based COFs family, but also demonstrated their application in immobilizing homogeneous metal-based (e.g., Rh-phosphine) catalysts for heterogeneous catalysis application.

## Introduction

Covalent organic frameworks (COFs) materials with porous crystalline structure assembled by covalent bonds<sup>[1]</sup> have attracted much attention in recent years because of their ordered pore structure, easy functionalization, high stability and low density. These materials have great potential applications in many fields such as gas storage, separation<sup>[2]</sup>, sensing<sup>[3]</sup>, energy conversion<sup>[4]</sup>, solid state ion conducting<sup>[5]</sup> and catalysis<sup>[6]</sup>. Since the first report on COFs in 2005<sup>[7]</sup>, a large number of structures have been designed and synthesized successfully. Yang *et al.* proposed a useful genomics method for high-throughput construction of COFs and established a library of 130 genetic structural units (GSUs) with a database of ca. 470,000 materials<sup>[8]</sup>. COFs are mainly functionalized by nitrogen-containing functional groups, such as triazine<sup>[9]</sup>, porphyrin<sup>[10]</sup> and Salen<sup>[11]</sup>. Very recently, great efforts have been devoted to synthesizing phosphine-based functional COFs due to the unique features of phosphine, e.g., in phosphine organocatalysis<sup>[12]</sup>. These attempts have used phosphine-containing building blocks, such as hexachlorocyclotriphosphazene<sup>[13]</sup>, triphenylphosphine (PPh<sub>3</sub>)<sup>[14]</sup>

and dibenzyl phosphite<sup>[15]</sup>, however, the obtained phosphine functionalized COFs show poor crystallinity<sup>[13,14]</sup> and more likely to be amorphous porous organic polymers (POPs)<sup>[15,16]</sup>. Conventionally, the planar tripodal sp<sup>2</sup> hybridized structural units tends to form a well-defined layered structure stabilized by  $\pi$ - $\pi$ -stacking interaction<sup>[1a,2a,17]</sup>. In contrast, a flexible sp<sup>3</sup>-hybridized unit, such as triphenylphosphine, tends to undergo a tetrahedral distortion due to repulsion from lone-pair of electrons. This interaction forces the unit to deviate from the planarity and twist to a smaller angle (<180°) between phenyl-propellers when forming two-dimensional structure, resulting in POPs materials<sup>[18]</sup>. In a paper recently published on-line, Tao *et al.*<sup>[19]</sup> successfully synthesized a first example of triphenylphosphine-based COFs, which presents both eclipsed AA stacking and staggered ABC stacking crystals in one sample, related to the trigonal pyramidal geometry of triphenylphosphine.

Herein, we report an improved synthesis of two examples of triphenylphosphine-based COFs (P-COFs, Scheme 1). These two P-COFs stack only in an AA eclipsed manner (*vide infra*) and have high crystallinity and specific surface areas, and good thermal stability. Considering that triphenylphosphine is a very important ligand for organometallic complexes (e.g., homogeneous Rh-phosphine based catalysts<sup>[20]</sup>), we further demonstrate here that P-COFs are superb support materials acting as promoters (ligands) as well for immobilization of homogeneous catalysts. Such heterogeneous P-COFs supported catalysts (e.g., Rh-P-COFs) have shown excellent catalytic activity, product selectivity and catalyst recyclability for hydroformylation of olefins (*vide infra*).



**Scheme 1.** Schematic representation of the synthesis of P-COFs.

[a] Dr. Y. Liu, N. Xu, J. Sun, J. Tang, K. Wang, Dr. B. Xu, Dr. Q. Tong, Prof. Dr. Y. Fan

Key Laboratory of Mesoscopic Chemistry of MOE, School of Chemistry and Chemical Engineering, Jiangsu Key Laboratory of Vehicle Emissions Control, Nanjing University, Nanjing 2100093, China  
E-mail: ynfan@nju.edu.cn

[b] Dr. A. Dikhtiarenko, Prof. Dr. J. Gascon  
KAUST Catalysis Center, Advanced Catalytic Materials, King Abdullah University of Science and Technology, Thuwal 23955, Saudi Arabia  
E-mail: jorge.gascon@kaust.edu.sa

[c] Prof. H.J. Heeres, Dr. S. He  
Green Chemical Reaction Engineering, University of Groningen, 9747 AG Groningen, The Netherlands  
E-mail: songbo.he@rug.nl

Supporting information for this article is given via a link at the end of the document.

## RESEARCH ARTICLE

## Results and Discussion

Two examples of imine-linked P-COFs were synthesized (SI, Section 2) through a Schiff base reaction of tris-(4-formylphenyl) phosphane (TFP, CAS No. 67753-41-7, synthesized according to references<sup>[21]</sup>) with *p*-phenylenediamine (PPD, CAS No. 106-50-3) or benzidine (CAS No. 92-87-5), denoted as P-COF-1 and P-COF-2, respectively (Scheme 1). To gain insight into the crystalline structure of the P-COFs, powder X-ray diffraction (PXRD) in combination with simulations were performed. The PXRD patterns of P-COF-1 and P-COF-2 (Figure 1a) exhibited an intense peak at  $2\theta = 4.2$  and  $3.4$ , individually, along with minor peaks at  $2\theta = 6.1, 7.3, 8.1, 12.1, 16.1$  for P-COF-1 and  $2\theta = 5.0, 6.1, 7.1, 10.0$  for P-COF-2. To elucidate the structure of P-COF-1 and calculate its unit cell parameters, several possible two-dimensional (2D) models with eclipsed and staggered stackings (Figures 1b and S1) were constructed and optimized applying geometrical energy minimization using a universal force-field method. Exploration of several possible models (Figures 1c and S1, Tables S1-S3) confirms that the best fit for the observed peaks, in both position and relative intensities, corresponding to 100, 110, 020 and 111 reflections of the eclipsed structure with an AA sequence of 2D layers. Comparison of experimental PXRD for P-COF-1 and P-COF-2 (Figure 1a) clearly evidences their isostructural characteristics. In addition, shifts in peak positions for P-COF-2 with respect to P-COF-1 are observed, indicating an enlargement of unit cell parameters for P-COF-2, as a result of extension of the ring units. Hence, we propose that both P-COF-1 and P-COF-2 structures stack in an AA eclipsed manner adopting hexagonal P6 settings and forming a system of open one-dimensional (1D) pore channels extended along the *c*-axis. This indicates that the developed syntheses in this submission

produce P-COF-s with higher purity, compared with the reported P-COF-1<sup>[19]</sup> crystals stacked in both eclipsed AA and staggered ABC manners. *Le Bail* refinements confirmed plausible assignment of the space group, as evidenced by the negligible difference between the simulated and experimental diffractograms for P-COF-1 (Figure S2) and P-COF-2 (Figure S3 and S4), yielding unit cell parameters of  $a = b = 32.55 \text{ \AA}$ ,  $c = 7.9 \text{ \AA}$  for P-COF-1 (Tables S1) and  $a = b = 40.35 \text{ \AA}$ ,  $c = 7.9 \text{ \AA}$  for P-COF-2 (Tables S4). The corresponding pore diameters for P-COF-1 and P-COF-2 were calculated to be  $37 \text{ \AA}$  and  $46 \text{ \AA}$ , respectively, with an interlayer separation of  $7.9 \text{ \AA}$ .

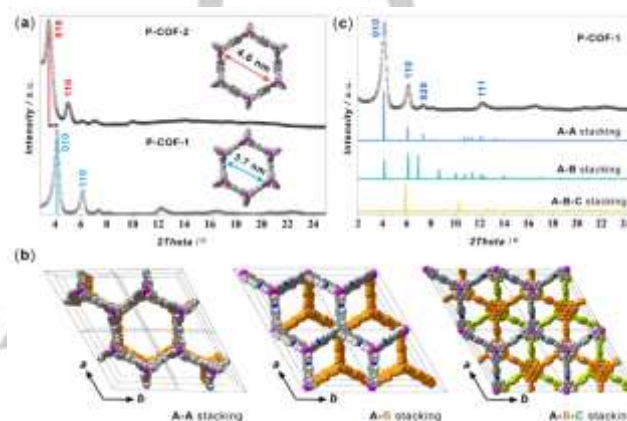


**Figure 1.** (a) Powder X-ray diffraction patterns of P-COF-1 and P-COF-2 revealed isostructural AA-stacking with different pore sizes. (b) The structural arrangement of AA, AB and ABC stackings in P-COF-1 viewed along *c*-axes. (c) PXRD pattern of P-COF-1 (black dots) compared to the simulated for AA eclipsed (blue curve, P6 space group), AB staggered (turquoise, P6<sub>3</sub> space group) and ABC staggered-interpenetrated (orange, R-3 space group) models

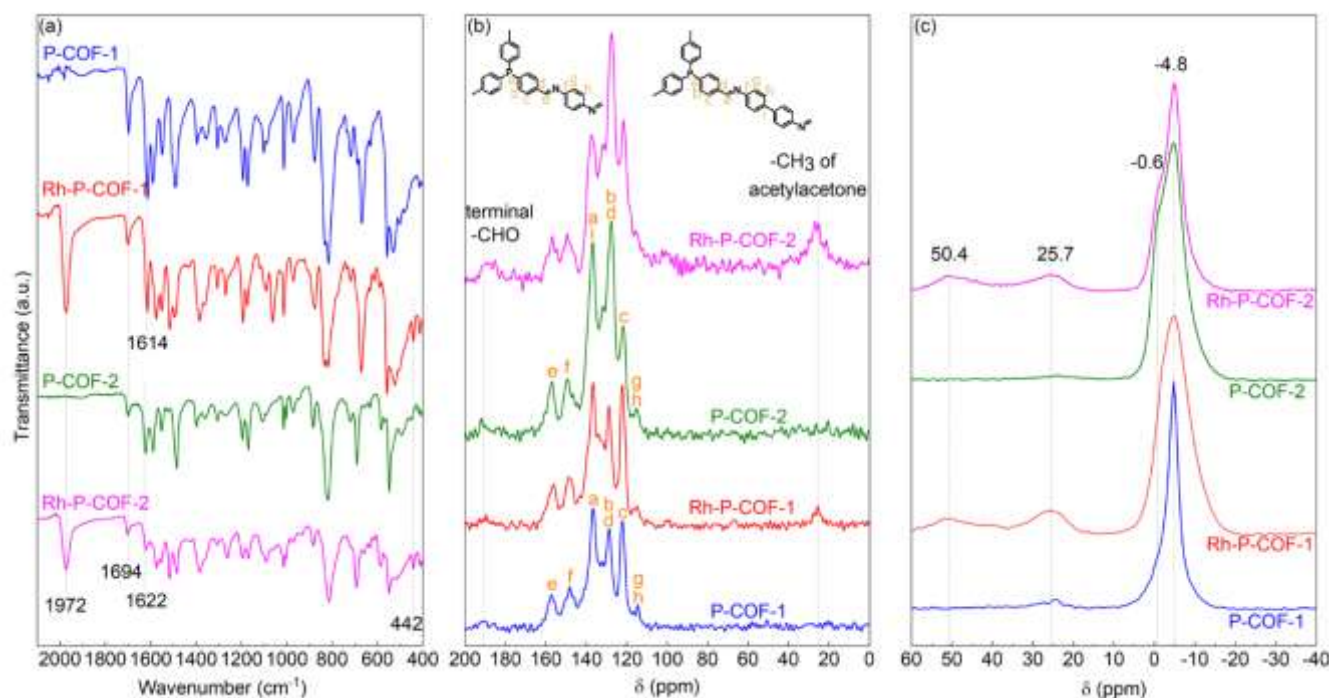


**Figure 2.** (a) FT-IR spectra, (b) <sup>13</sup>C CP-MAS ssNMR and (c) <sup>31</sup>P static ssNMR of P-COFs and Rh-P-COFs.

## RESEARCH ARTICLE

The C=N bonds in the P-COFs are formed by the condensation of aldehyde groups of TFP with the amino groups of *p*-phenylenediamine or benzidine<sup>[22]</sup>, resulting in the disappearance of the N-H bonds, as evidenced by the diminished N-H stretching bands at 3100-3400 cm<sup>-1</sup> for *p*-phenylenediamine (Figure S5) and benzidine (Figure S6). A relatively weak C=O stretching band at 1694 cm<sup>-1</sup> was still present in the FT-IR spectra of P-COFs (Figure 2a), probably because of the presence of residual terminal aldehyde groups of TFP at the terminal edges of the P-COFs (Figures S5 and S6)<sup>[4b, 23]</sup>. <sup>13</sup>C CP-MAS solid-state NMR spectra of the P-COFs (Figure 2b) show characteristic resonances for the C atom of a C=N moiety located at  $\delta = 156$  ppm<sup>[24]</sup>, consistent with Fourier transform infrared (FT-IR) spectra of the P-COFs (Figure 2a, with C=N stretching bands at 1614 and 1622 cm<sup>-1</sup> for P-COF-1 and P-COF-2, respectively). <sup>31</sup>P static solid-state NMR spectra of the P-COFs (Figure 2c) show a single sharp peak at  $\delta = -4.8$  ppm in line with that for TFP (Figure S8). There is a presence of a little collar around  $\delta = -0.6$  ppm in P-COF-2, which may represent P-COF-2 with different polymerization degree from that of  $\delta = -4.8$  ppm.

Scanning electron microscopy (SEM, Figure 3) images of P-COFs show the microspheric crystals with urchin-like surface morphology, which might be considered as the result of aggregation of a large number of nanosheets (Figure S9) formed by  $\pi$ - $\pi$  stacking of P-COF layers<sup>[25]</sup>.

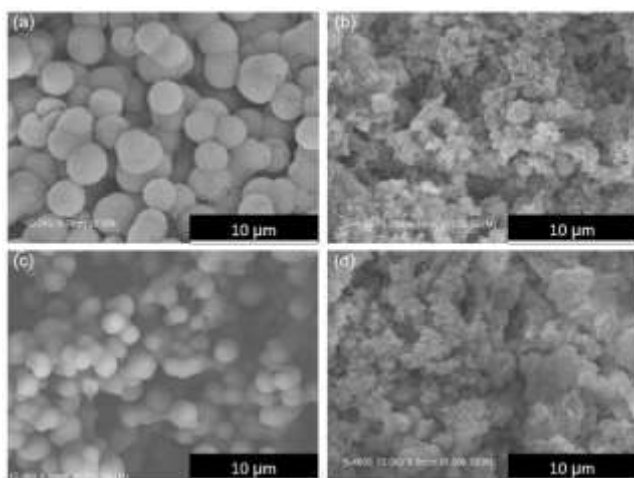


**Figure 3.** SEM images of (a) P-COF-1, (b) P-COF-2, (c) Rh-P-COF-1 and (d) Rh-P-COF-2.

Adsorption/desorption of Ar and N<sub>2</sub> (Figure 4, S11) were performed to characterize the pore structure of P-COFs. N<sub>2</sub> adsorption/desorption isotherms of P-COFs (Figure S10a) show the combined characteristics of Type I and Type IV<sup>[26]</sup>, indicating the microporous ( $P/P_0 < 0.1$ ) and mesoporous ( $0.4 < P/P_0 < 1$ ) structure. The pore size distributions (PSDs) of the P-COFs (Figure 4), calculated on the basis of the nonlocal density functional theory (NLDFT)<sup>[27]</sup>, show a wide pore distribution in the range of 2-25 nm for P-COFs. The Brunauer-Emmett-Teller (BET) surface areas based on nitrogen adsorption/desorption isotherms

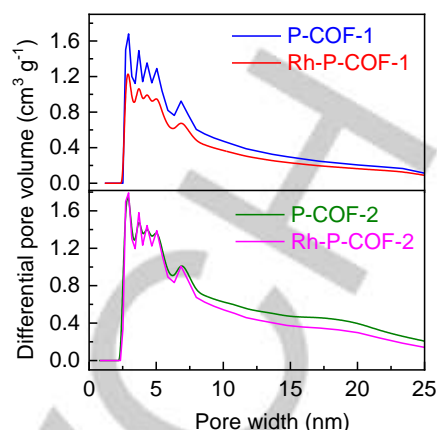


**Figure 4.** NLDFT pore size distribution from Ar adsorption of P-COFs and Rh-P-COFs.

of the P-COFs are 903 m<sup>2</sup> g<sup>-1</sup> (P-COF-1, close to the S<sub>BET</sub> for the reported P-COF-1<sup>[19]</sup>) and 2387 m<sup>2</sup> g<sup>-1</sup> (P-COF-2). And the corresponding total pore volumes are 0.69 cm<sup>3</sup> g<sup>-1</sup> (P-COF-1) and 4.22 cm<sup>3</sup> g<sup>-1</sup> (P-COF-2). Notably, these surface areas of triphenylphosphine-based COFs are higher than those for amorphous triphenylphosphine-based POPs<sup>[18]</sup>.

Both P-COFs show good thermal stability under inert atmosphere, which is evidenced by the negligible weight loss up to 450 °C under N<sub>2</sub> atmosphere during thermo-gravimetric analysis (TGA, Figure 5) and the well-retained crystallinities up to 300 °C under vacuum during the in-situ variable temperature PXRD (in-situ VT-PXRD, Figure 5) analysis<sup>[28]</sup>. In addition, the P-COFs are insoluble in water and common organic solvents such as acetone, ethanol, hexane, *N,N*-dimethylformamide (DMF) and tetrahydrofuran (THF). To examine the chemical stability of P-COFs<sup>[29]</sup>, the samples were exposed to different chemical environments for 24 h, including tetrahydrofuran (THF), DMF, ethanol, boiling water, HCl (aq) (pH=1), concentrated HCl (4 M), NaOH (aq) (pH=14), and concentrated NaOH (4M). P-COF-1 and P-COF-2 retain their original skeleton and crystalline structure after treatment in THF, DMF, and ethanol, as indicated by well-kept PXRD patterns (Figure S11). Comparatively, P-COF-1 has better stability in boiling water and NaOH (aq) than P-COF-2. Both P-COF-1 and P-COF-2 lost their crystallinity after acidic medium treatment, likely related to the hydrolytic nature of the imine bonds, which was also observed for other imine-linked COFs<sup>[6b,11]</sup>.

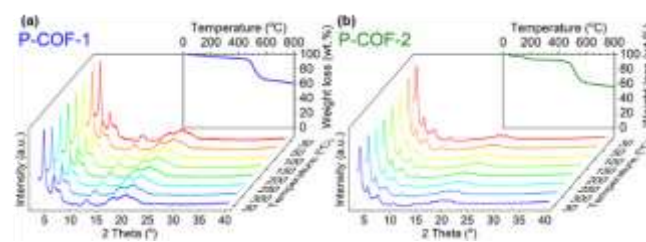


**Figure 5.** In-situ VT-PXRD patterns (under vacuum) and TGA curves (under N<sub>2</sub>) of P-COFs.

## RESEARCH ARTICLE

Extending the novelty and promising structures of P-COFs, both P-COFs have been used as support materials containing triphenylphosphine ligands for the immobilization of metal complex catalysts. To demonstrate this, an easy post-treatment (SI, Section S2.3) of two P-COFs with (acetylacetonato)dicarbonylrhodium (I) ( $\text{Rh}(\text{CO})_2(\text{acac})$ ) was performed. After Rh loading, the morphology of P-COFs was maintained, as shown by SEM (Figure 3) and TEM (Figure S9). Those typical diffraction peaks for P-COFs were preserved, indicated by PXRD (Figure 6). In addition, diffraction peaks for  $\text{Rh}(\text{CO})_2(\text{acac})$  were not observed on both Rh-P-COFs. However, the lattice fringes of Rh (111) plane with ca. 0.26 nm spacing can be observed on Rh-P-COF-1 treated by  $\text{NaBH}_4$  (Figure S10). These results indicated that the  $\text{Rh}(\text{CO})_2(\text{acac})$  is uniformly distributed on Rh-P-COFs, in accordance with the SEM-EDS mapping (Figure S13) of the Rh-P-COFs. FT-IR spectra of Rh-P-COFs (Figure 2a) show the terminal CO stretching vibration  $\nu_{\text{CO}}$  at  $1972\text{ cm}^{-1}$ <sup>[30]</sup>, which is different from those of  $\text{Rh}(\text{CO})_2(\text{acac})$  (Figure S14) showing the symmetric and asymmetric  $\nu_{\text{CO}}$  at  $2062\text{ cm}^{-1}$  and  $1993\text{ cm}^{-1}$ , respectively<sup>[31]</sup>. In addition, an absorption band at  $442\text{ cm}^{-1}$  was observed for Rh-P-COFs (Figure 2a), attributed to Rh-P vibration, indicating a coordination bond between Rh and P<sup>[32]</sup>. This was further confirmed by  $^{31}\text{P}$  static solid-state NMR spectra for both Rh-P-COFs (Figure 2c), which exhibited two new resonances at  $\delta = \text{ca. } 25\text{ ppm}$  and  $\delta = \text{ca. } 50\text{ ppm}$ , assigned to oxidized species  $\text{P}=\text{O}$  and P atoms coordinated with Rh, respectively<sup>[33]</sup>. Furthermore, X-ray photoelectron spectroscopy (XPS) spectra show that in the Rh  $3d_{5/2}$  band (Figure 7a) there are two peak at binding energy (BE) of 308.3 eV and 308.5 eV for Rh-P-COFs, which is slightly lower than for the parent  $\text{Rh}(\text{CO})_2(\text{acac})$  (309.3 eV). The binding energies of the P  $2p_{3/2}$  band in Rh-P-COFs (131.8 eV) are higher than that in P-COFs (130.6 eV) (Figure 7b), attributed to electron transfer from P to Rh<sup>[18a, 33a]</sup>, resulting in more electron-rich Rh atoms in the Rh-P-COFs. Meanwhile, the electron may also transfer from N to Rh, indicated by the binding energies of the N 1s band (Figure S15) for Rh-P-COFs (400.0 eV) and P-COFs (398.9 eV). The peak at 132.5 eV (Figure 7b) might be attributed to oxidized phosphorus atoms ( $\text{P}=\text{O}$ )<sup>[34]</sup>. Nevertheless, the current study could not illustrate the coordination mode of Rh with P-COFs and the distribution of Rh (e.g., on crystal surface or in the matrix), which

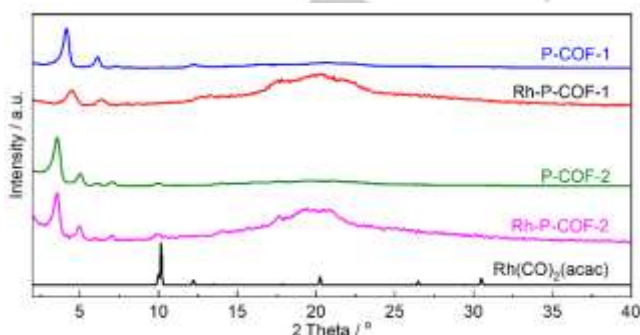


Figure 6. PXRD patterns of P-COFs, Rh-P-COFs and  $\text{Rh}(\text{CO})_2(\text{acac})$ .

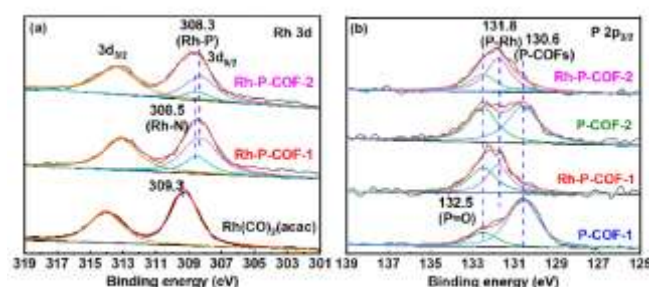


Figure 7. XPS of (a) Rh 3d and (b) P  $2p_{3/2}$  for  $\text{Rh}(\text{CO})_2(\text{acac})$ , P-COFs and Rh-P-COFs.

is very challenging and requires a further investigation with multiple techniques.

The Rh-P-COFs were employed as heterogeneous catalysts for hydroformylation of olefins<sup>[20b]</sup> under an optimized P/Rh ratio (Figure S16), reaction temperature (Figure S17) and reaction time (Figure S18). Initial experiments of hydroformylation of styrene were performed with two homogeneous catalysts, viz.  $\text{Rh}(\text{CO})_2(\text{acac})$  and  $\text{Rh}(\text{CO})_2(\text{acac})$  in combination with  $\text{P}(\text{Ph})_3$ . It was found (Table 1) that the latter indeed shows a higher turnover frequency (TOF,  $3302\text{ h}^{-1}$ ) and aldehyde selectivity (96 %) than the only  $\text{Rh}(\text{CO})_2(\text{acac})$  ( $1368\text{ h}^{-1}$  and 90%, respectively). As expected, the heterogeneous Rh-P-COFs catalysts show higher TOFs ( $2557\text{ h}^{-1}$  for Rh-P-COF-1 and  $2074\text{ h}^{-1}$  for Rh-P-COF-2, Table 1) and aldehyde selectivity (94% for Rh-P-COF-1 and 96 % for Rh-P-COF-2, Table 1) than homogeneous  $\text{Rh}(\text{CO})_2(\text{acac})$  catalyst. When prolonging the reaction time to 6 h, the olefin conversion over Rh-P-COFs reaches 95 % (Figure S18). These promising catalytic conversion and product selectivity were also obtained for hydroformylation of other olefins, e.g., 1-Hexene, 1-Octene, 4-Methoxystyrene and 4-Chlorostyrene (Table S7). Furthermore, the reusability of the heterogeneous Rh-P-COFs catalysts were investigated by filtrating the used Rh-P-COFs catalysts and recycling several times. Similar olefin conversions

Table 1. Hydroformylation of styrene over homogeneous  $\text{Rh}(\text{CO})_2(\text{acac})$  without/with  $\text{P}(\text{Ph})_3$  ligands and over the heterogeneous Rh-P-COFs catalysts.<sup>a</sup>

Catalyst	Conversion (mol%)	Selectivity of aldehydes (mol%)	Regioselectivity <sup>b</sup>	TOF <sup>c</sup> ( $\text{h}^{-1}$ )
$\text{Rh}(\text{CO})_2(\text{acac})$	19	90	0.9	1368
$\text{Rh}(\text{CO})_2(\text{acac})$ + $\text{P}(\text{Ph})_3$	43	96	0.6	3302
Rh-P-COF-1 (fresh)	34	94	0.9	2557
Rh-P-COF-2 (fresh)	27	96	1.1	2074
Rh-P-COF-1 (6th recycled)	31	97	1.1	2398
Rh-P-COF-2 (6th recycled)	27	94	1.0	2050

<sup>a</sup>Reaction conditions: Rh dose 0.0023 mmol, molar ratio of P/Rh ca. 4.0, molar ratio of S/C (substrate/catalyst) of ca. 2000,  $\text{CO}:\text{H}_2 = 1:1$ ,  $t = 0.25\text{ h}$ ,  $P = 2.0\text{ MPa}$ ,  $T = 100\text{ }^\circ\text{C}$  and 4 mL toluene.

<sup>b</sup>Regioselectivity: molar ratio of linear (*n*-) aldehydes/branched (*iso*-) aldehydes.

## RESEARCH ARTICLE

after 6 h reaction was achieved over 5 cycles (Figure S19), with a small drop in aldehyde selectivity (Figure S19 and Table 1). Rh contents in the liquid products, analyzed by the inductively coupled plasma optical emission spectroscopy (ICP-OES), indicate that there is no leaching of Rh active metal species. The limited decrease of the TOF for the 6th recycled Rh-P-COF-1 (ca. 6.2 %) and Rh-P-COF-2 (ca. 1.2 %) compared to the corresponding fresh Rh-P-COFs (Table 1) indicates an excellent reusability of the Rh-P-COFs catalysts.

## Conclusion

In summary, we have demonstrated the synthesis of two examples of high crystalline and porous triphenylphosphine-based covalent organic framework (P-COFs) through a Schiff base reaction. Both P-COF-1 and P-COF-2 adopt an AA-stacking to form accessible open channels of 37 Å and 46 Å, respectively. The P-COFs supported Rh(CO)<sub>2</sub>(acac) catalysts (Rh-P-COFs) via Rh-P coordination bonds show high TOF (> 2000 h<sup>-1</sup>), high aldehyde selectivity (ca. 99 %) and excellent catalyst reusability (> 5 cycles) for hydroformylation of olefins. We believe that the novel triphenyl phosphine-based COFs are not only suitable to immobilize homogeneous metal-based catalysts but also have the important potential applications in other fields such as adsorption-separation, electrocatalysis and photocatalysis.

## Acknowledgements

Y. Liu and Y. Fan thank National Natural Science Foundation of China (NSFC), S. He and H.J. Heeres thank Netherlands Organization for Scientific Research (NWO) for their financial support (NSFC Grant No. 21773107 and NWO-LIFT Programme Grant No.731.016.401) to this work.

**Keywords:** covalent organic frameworks • triphenylphosphine • olefin hydroformylation • recyclable heterogeneous catalyst

- [1] a) N. Huang, P. Wang, D. Jiang, *Nat. Rev. Mater.* **2016**, 1; b) F. Beuerle, B. Gole, *Angew. Chem. Int. Ed.*, **2018**, 57, 4850-4878; c) D. Jiang, X. Chen, K. Geng, R. Liu, K. T. Tan, Y. Gong, Z. Li, S. Tao, Q. Jiang, *Angew. Chem. Int. Ed.*, **2020**, doi:10.1002/anie.201904291.
- [2] a) H. Fan, A. Mundstock, A. Feldhoff, A. Knebel, J. Gu, H. Meng, J. Caro, *J. Am. Chem. Soc.* **2018**, 140, 10094-10098; b) P. Wang, X. Chen, Q. Jiang, M. Addicoat, N. Huang, S. Dalapati, T. Heine, F. Huo, D. Jiang, *Angew. Chem. Int. Ed.*, **2019**, 58, 15922-15927.
- [3] a) Z. Li, N. Huang, K. H. Lee, Y. Feng, S. Tao, Q. Jiang, Y. Nagao, S. Irlé, D. Jiang, *J. Am. Chem. Soc.* **2018**, 140, 12374-12377; b) H. Singh, V. K. Tomer, N. Jena, I. Bala, N. Sharma, D. Nepak, A. De Sarkar, K. Kailasam, S. K. Pal, *J. Mater. Chem. A* **2017**, 5, 21820-21827.
- [4] a) J. Thote, H. B. Aiyappa, A. Deshpande, D. Diaz Diaz, S. Kurungot, R. Banerjee, *Chem. - Eur. J.* **2014**, 20, 15961-15965; b) V. S. Vyas, F. Haase, L. Stegbauer, G. Savasci, F. Podjaski, C. Ochsenfeld, B. V. Lotsch, *Nat. Commun.* **2015**, 6, 8508; c) J. Lv, Y.-X. Tan, J. Xie, R. Yang, M. Yu, S. Sun, M.-D. Li, D. Yuan, Y. Wang, *Angew. Chem. Int. Ed.*, **2018**, 57, 12716-12720.
- [5] a) Q. Xu, S. Tao, Q. Jiang, D. Jiang, *J. Am. Chem. Soc.* **2018**, 140, 7429-7432; b) H. Xu, S. Tao, D. Jiang, *Nat. Mater.* **2016**, 15, 722.
- [6] a) Q. Sun, Y. Tang, B. Aguila, S. Wang, F.-S. Xiao, P. K. Thallapally, A. M. Al-Enizi, A. Nafady, S. Ma, *Angew. Chem. Int. Ed.*, **2019**, 58, 8670-8675; b) S.-Y. Ding, J. Gao, Q. Wang, Y. Zhang, W.-G. Song, C.-Y. Su, W. Wang, *J. Am. Chem. Soc.* **2011**, 133, 19816-19822. c) Q. Fang, S. Gu, J. Zheng, Z. Zhuang, S. Qiu, Y. Yan, *Angew. Chem. Int. Ed.*, **2014**, 53, 2878-2882.
- [7] A. P. Côté, A. I. Benin, N. W. Ockwig, M. Keeffe, A. J. Matzger, O. M. Yaghi, *Science* **2005**, 310, 1166.
- [8] Y. Lan, X. Han, M. Tong, H. Huang, Q. Yang, D. Liu, X. Zhao, C. Zhong, *Nat. Commun.* **2018**, 9, 5274.
- [9] K. Kamiya, R. Kamai, K. Hashimoto, S. Nakanishi, *Nat. Commun.* **2014**, 5, 5040.
- [10] G. Lin, H. Ding, R. Chen, Z. Peng, B. Wang, C. Wang, *J. Am. Chem. Soc.* **2017**, 139, 8705-8709.
- [11] L.-H. Li, X.-L. Feng, X.-H. Cui, Y.-X. Ma, S.-Y. Ding, W. Wang, *J. Am. Chem. Soc.* **2017**, 139, 6042-6045.
- [12] H. Guo, Y. C. Fan, Z. Sun, Y. Wu, O. Kwon, *Chem. Rev.* **2018**, 118, 10049-10293.
- [13] M. Zhang, Y. Li, C. Bai, X. Guo, J. Han, S. Hu, H. Jiang, W. Tan, S. Li, L. Ma, *ACS Appl. Mater. Inter.* **2018**, 10, 28936-28947.
- [14] P. J. C. Hausoul, T. M. Eggenhuisen, D. Nand, M. Baldus, B. M. Weckhuysen, R. J. M. Klein Gebbink, P. C. A. Bruijninx, *Catal. Sci. Technol.* **2013**, 3, 2571-2579.
- [15] S. Ravi, P. Puthiaraj, K. Yu, W.-S. Ahn, *ACS Appl. Mater. Inter.* **2019**, 11, 11488-11497.
- [16] J. Huang, J. Tarábek, R. Kulkarni, C. Wang, M. Dračinský, G. J. Smales, Y. Tian, S. Ren, B. R. Pauw, U. Resch-Genger, M. J. Bojdys, *Chem. - Eur. J.* **2019**, 25 (53), 12342-12348.
- [17] Y. L. Zhu, S. Wan, Y. H. Jin, W. Zhang, *J. Am. Chem. Soc.* **2015**, 137, 13772-13775.
- [18] a) Q. Sun, Z. F. Dai, X. L. Liu, N. Sheng, F. Deng, X. J. Meng, F. S. Xiao, *J. Am. Chem. Soc.* **2015**, 137, 5204-5209; b) K. Dong, Q. Sun, Y. Q. Tang, C. Shan, B. Aguila, S. Wang, X. J. Meng, S. Q. Ma, F. S. Xiao, *Nat. Commun.* **2019**, 10.
- [19] Tao, R., Shen, X. R., Hu, Y. M., Kang, K., Zheng, Y. Q., Luo, S. C., Yang, S. Y., Li, W. L., Lu, S. L., Jin, Y. H., Qiu, L., Zhang, W., *Small* **2020**, doi:10.1002/sml.201906005.
- [20] a) H. Guo, Y. C. Fan, Z. Sun, Y. Wu, O. Kwon, *Chem. Rev.* **2018**, 118, 10049-10293; b) R. Franke, D. Selent, A. Borner, *Chem. Rev.* **2012**, 112, 5675-5732.
- [21] a) H. Nishi, T. Namari, S. Kobatake, *J. Mater. Chem.* **2011**, 21, 17249-17258; b) F. Chalier, Y. Berchadsky, J.-P. Finet, G. Gronchi, S. Marque, P. Tordo, *J. Phys. Chem.* **1996**, 100, 4323-4330.
- [22] a) P. J. Waller, Y. S. AlFaraj, C. S. Diercks, N. N. Jarenwattananon, O. M. Yaghi, *J. Am. Chem. Soc.* **2018**, 140, 9099-9103; b) G. Zhang, M. Tsujimoto, D. Packwood, N. T. Duong, Y. Nishiyama, K. Kadota, S. Kitagawa, S. Horike, *J. Am. Chem. Soc.* **2018**, 140, 2602-2609.
- [23] C. Qian, S.-Q. Xu, G.-F. Jiang, T.-G. Zhan, X. Zhao, *Chem. - Eur. J.* **2016**, 22, 17784-17789.
- [24] a) X. Wang, X. Han, J. Zhang, X. Wu, Y. Liu, Y. Cui, *J. Am. Chem. Soc.* **2016**, 138, 12332-12335; b) G. Lin, H. Ding, D. Yuan, B. Wang, C. Wang, *J. Am. Chem. Soc.* **2016**, 138, 3302-3305.
- [25] S. Karak, S. Kandambeth, B. P. Biswal, H. S. Sasmal, S. Kumar, P. Pachfule, R. Banerjee, *J. Am. Chem. Soc.* **2017**, 139, 1856-1862.
- [26] K. S. W. Sing, D. H. Everett, R. A. W. Haul, L. Moscou, R. A. Pierotti, J. Rouquerol, T. Siemieniowska, *Pure Appl. Chem.* **1985**, 57, 603-619.
- [27] F. J. Uribe-Romo, J. R. Hunt, H. Furukawa, C. Klock, M. O'Keeffe, O. M. Yaghi, *J. Am. Chem. Soc.* **2009**, 131, 4570-4571.
- [28] Q. Liao, C. Ke, X. Huang, G. Zhang, Q. Zhang, Z. Zhang, Y. Zhang, Y. Liu, F. Ning, K. Xi, *J. Mater. Chem. A* **2019**, 7 (32), 18959-18970.
- [29] a) S. Kandambeth, A. Mallick, B. Lukose, M. V. Mane, T. Heine, R. Banerjee, *J. Am. Chem. Soc.* **2012**, 134, 19524-19527; b) X. Han, Q. Xia, J. Huang, Y. Liu, C. Tan, Y. Cui, *J. Am. Chem. Soc.* **2017**, 139, 8693-8697.
- [30] J. Zhang, M. Poliakoff, M. W. George, *Organometallics* **2003**, 22, 1612-1618.

## RESEARCH ARTICLE

- [31] A. M. F. Brouwers, A. Oskam, R. Narayanaswamy, A. J. Rest, *J. Chem. Soc., Dalton Trans.* **1982**, 1777-1782.
- [32] H. G. M. Edwards, A. F. Johnson, I. R. Lewis, *Spectrochim. Acta, Part A.* **1993**, 49, 707-714.
- [33] a) C. Li, L. Yan, L. Lu, K. Xiong, W. Wang, M. Jiang, J. Liu, X. Song, Z. Zhan, Z. Jiang, Y. Ding, *Green Chem.* **2016**, 18, 2995-3005; b) W. Wang, C. Li, L. Yan, Y. Wang, M. Jiang, Y. Ding, *ACS Catal.* **2016**, 6, 6091-6100.
- [34] J. R. Blackburn, R. Nordberg, F. Stevie, R. G. Albridge, M. M. Jones, *Inorg. Chem.* **1970**, 9, 2374-2376.

WILEY-VCH

Accepted Manuscript

## RESEARCH ARTICLE

## Entry for the Table of Contents

## RESEARCH ARTICLE

Two examples of triphenylphosphine-based COFs (P-COFs), which stack in an eclipsed AA manner and have high crystallinity, high specific surface areas and good thermal stability, have been successfully synthesized. The application of these two P-COFs in phosphorus coordination catalysis has been demonstrated by hydroformylation of olefins over the supported Rh/P-COFs catalysts, showing high TOF and excellent recycling performance.



Yubing Liu, Alla Dikhtiarenko, Naizhang Xu, Jiawei Sun, Jie Tang, Kaiqiang Wang, Bolian Xu, Qing Tong, Hero Jan Heeres, Songbo He\*, Jorge Gascon\* and Yining Fan\*

Page No. – Page No.

The Triphenylphosphine-Based Covalent Organic Frameworks

Accepted Manuscript